Available online at www.sciencedirect.com
SCIENCE DIRECT®
International Journal of Heat and Mass Transfer 47 (2004) 601–612
International Journal of HEAT and MASS TRANSFER
www.elsevier.com/locate/ijhmt

Dissolution and solutal convection in partially miscibile liquid systems

Raffaele Savino [a,*], Marcello Lappa [b]

[a] Dipartimento di Scienza e Ingegneria dello Spazio "Luigi G. Napolitano", Università degli Studi di Napoli "Federico II", P.le V.Tecchio 80, 80125 Napoli, Italy

[b] MARS Center (Microgravity Advanced Research and Support Center), Via Emanuele Gianturco 31, 80142 Napoli, Italy

Received 3 January 2003

Abstract

A numerical model is developed to study the dissolution of droplets in a binary mixture with miscibility gap. The moving boundary problem is solved with a modified volume of fraction method to compute the time evolution of the average drop radius and the velocity and concentration distributions around the dissolving drop. The modeling results are presented to explain experimental findings that show stable and oscillatory plumes rising from droplets of methanol that dissolve into a cyclohexane liquid matrix.

1. Introduction

In recent years binary liquid–liquid systems, and particularly partially miscible liquid pairs, have been finding increasing applications in fundamental studies of interphase mass transfer. For instance, transparent liquids are often used as models for the investigation of the behaviour of metal alloys in the liquid state. Typically these alloys are solidified from a homogeneous binary mixture into regions of their phase diagrams with a miscibility gap [1]. The formed two-phase liquid consists of dispersed drops in a matrix liquid. Since the materials properties can be improved by a uniform dispersion of fine particles in the primary phase, the quality of the metal alloys depends on the degree of homogeneity of the minority phase distribution.

During alloys solidification, the melt is subject to temperature and concentration gradients that, in the gravity field, lead in most cases to buoyancy driven convective flows. Moreover, as the phase concentrations are different, the minority phase may experience buoyancy or sedimentation [2].

Due to major difficulties in investigating liquid metals at high temperatures (toxicity, reactivity, opaqueness), organic liquids are often used as model substances to study mixing and separation. For instance, methanol and cyclohexane have been investigated both on earth and in space since they are transparent liquids at ambient temperature. They exhibit a miscibility gap in the phase diagram and have a relatively small difference in density (0.769 g/cm^3 the cyclohexane, 0.782 g/cm^3 the methanol). In principle, this allows minimization of buoyancy and sedimentation effects.

One basic problem to be studied is the migration of droplets imbedded in a different fluid in the presence of a temperature gradient, and gravitational effects (see e.g. [3]). Furthermore, the issues of coalescence, growth and disappearance of droplets during the phase separation processes are of basic importance [1].

In preparation of microgravity experiments the dissolution process has been investigated under normal gravity conditions.

A droplet of methanol was formed on the tip of a capillary immersed into the cyclohexane to study the droplet dissolution. The experimental procedure includes the visual observation of the droplet and an interferometric analysis performed with a Wollaston optical system, to analyze the concentration field and therefore the mass transfer at the binary liquid–liquid interface.

* Corresponding author.

0017-9310/$ - see front matter © 2003 Elsevier Ltd. All rights reserved.
doi:10.1016/S0017-9310(03)00337-5

Nomenclature

c	mass concentration
D	diffusion coefficient [m^2/s]
g	gravity acceleration (9.81 m/s^2)
i	ith grid point of the mesh in the x direction
j	jth grid point of the mesh in the y direction
n	normal coordinate [m]
$\underline{\hat{n}}$	unit perpendicular to the interface
P	pressure [Pa]
r	distance from the drop center [m]
R	drop radius [m]
T	temperature [K]
t	time [s]
$\underline{V}$	velocity vector [m/s]
x, y	cartesian coordiantes [m]
Greek symbols	
ρ	density [kg/m^3]
$\underline{\nabla}$	Nabla operator [1/m]
∇^2	Laplace operator [1/m^2]
μ	dinamic viscosity [kg/m/s]
β	solutal expansion coefficient
ϕ	phase field variable (1 for droplet phase, 0 for matrix phase)
Δt	time step [s]
Δx	size of the grid cell in the x direction [m]
Subscripts	
1	drop liquid
2	matrix liquid
(e)	equilibrium interface conditions
m	matrix concentration far away from the interface
0	initial condition

In spite of the small differences in density between the droplet and the surrounding matrix, a convective motion is evident in the experimental cell, causing a strong distortion of the concentration distribution (compared to the purely diffusive situation). Furthermore, the plume, originated at the tip of the drop and directed upwards, exhibits in some cases pronounced regular oscillations that reveal a convective instability of the oscillatory type.

In previous experiments with different liquid–liquid systems (aniline/water, isobutanol/water, ethilacetate/water, see [4]) similar convective plumes become unstable due to Marangoni effects induced by surfactants. In the above mentioned studies, the systems basically consisted of sitting droplets (if the droplet liquid is lighter than that of the matrix) or of pendant droplets (if the droplet liquid is heavier than that of the matrix). Correspondingly, the convective plume is directed downward (for pendant droplet) or upwards (for sitting droplet). In the system under investigation, even though the droplet (methanol) is heavier than the surrounding matrix (cyclohexane), the plume is directed upwards and, in many cases, the flow and concentration fields at the dissolving interface exhibit periodic oscillations.

The objective of this paper is to provide a theoretical explanation of the observed phenomena with a numerical model to study the droplet dissolution process.

2. Experiments

The experiments have been performed with a Wollaston interferometer, using a Hellma cell made of quartz, 1 [cm]×1 [cm]×4 [cm], filled with liquid. A droplet of a liquid partially miscible with that of the matrix (volume ranging from 1 to 5 μl) was formed at the tip of a capillary (1 mm diameter), as shown in Fig. 1. The temperatures at the top and bottom walls are controlled by Peltier elements. In this system the droplet liquid is denoted as phase 1 and the liquid matrix as phase 2.

Fig. 2 shows an image of a droplet of butanol dissolving in water. Since the butanol is lighter than water ($\rho_1 = 0.81$ g/cm^3; $\rho_2 = 1$ g/cm^3), the interference fringes

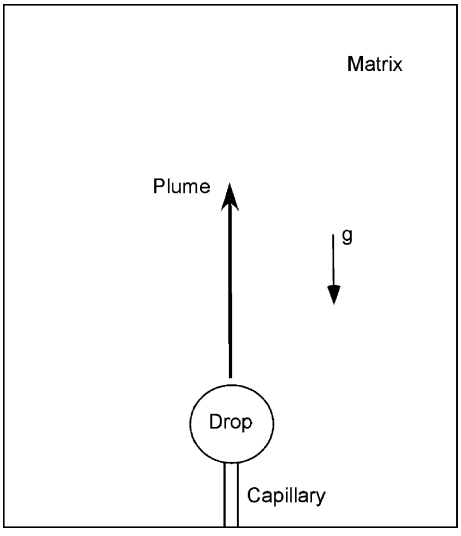

Fig. 1. Sketch of the geometrical configuration.

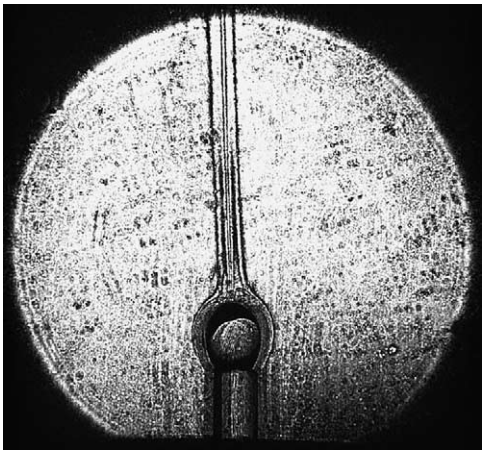

Fig. 2. Rising plume from a droplet of butanol dissolving in water at ambient temperature (initial drop volume of 1.5 μl).

show a convective plume originated at the dissolving interface and directed upwards. Fig. 3 shows the behaviour of a droplet of methanol in a matrix of hexane. In this case the drop liquid is heavier than the matrix liquid ($\rho_1 = 0.782$ g/cm^3; $\rho_2 = 0.65$ g/cm^3) so that the flow around the droplet, shown by the interference pattern, is directed downward.

Fig. 4 shows a dissolving drop of methanol in cyclohexane. As explained before, the drop liquid is heavier than the matrix ($\rho_1 = 0.782$ g/cm^3; $\rho_2 = 0.769$ g/cm^3) so one should expect a behaviour similar to that of Fig. 3. On the contrary, a convective plume originates at the dissolving interface directed upwards, similar to the case illustrated in Fig. 2.

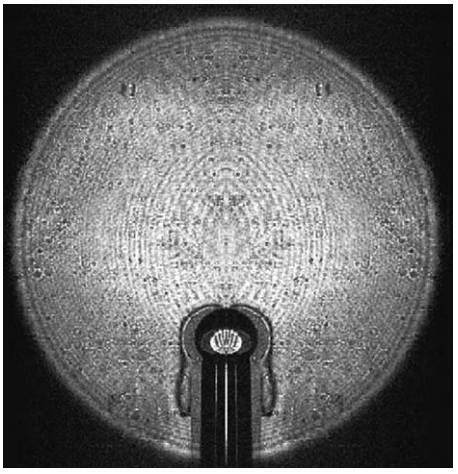

Fig. 3. Descending flow from a droplet of methanol dissolving in hexane at ambient temperature (initial drop volume of 1.5 μl).

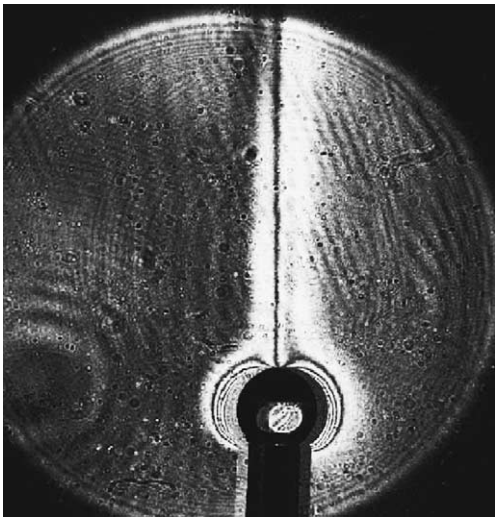

Fig. 4. Rising plume from a droplet of methanol dissolving in cyclohexane at ambient temperature (initial drop volume of 3 μl).

This phenomenon can be explained by the density of the cyclohexane–methanol system as a function of the concentration. When a drop of pure methanol is injected into the cyclohexane liquid matrix, equilibrium at the liquid–liquid interface is attained instantaneously [5]. Assuming negligible thermal effects (temperature differences less than 0.2 °C were measured with thermocouples), according to the phase rule, the concentrations at the interface will be $c_{1(e)}$ and $c_{2(e)}$ (inside and outside the droplet, respectively), i.e. the equilibrium methanol concentrations at the consolute points of the miscibility diagram, see Fig. 5a. According to [6], the density of the binary mixture is a decreasing function of the methanol concentration for $0 < c < c_{2(e)}$, and an increasing function for $c_{1(e)} < c < 1$ (see Fig. 5b). Correspondingly the mixture surrounding the droplet is lighter than the external matrix and therefore a rising plume is formed.

The time evolution of the average droplet radius was measured for different initial volumes and at different temperatures. Typical results obtained at ambient temperature are shown in Fig. 6, for the case of a droplet with initial volume of 3 μl. The experimental results are compared with the results of numerical simulations (see next section) under zero-gravity and normal gravity conditions. In the purely diffusive situation (zero-g), the droplet radius decreases proportional with the square root of time, according to the analytical solution [1] $R^2 = R_0^2 - D\frac{c_m - c_{2(e)}}{c_{2(e)} - c_{1(e)}}t$, where D is the diffusion coefficient, c_m is the matrix concentration (far away from the interface). In the presence of the gravity acceleration, the main effect of the convective motion around the dissolving drop is to change the concentration distribution. As will be discussed below, the isoconcentration lines are

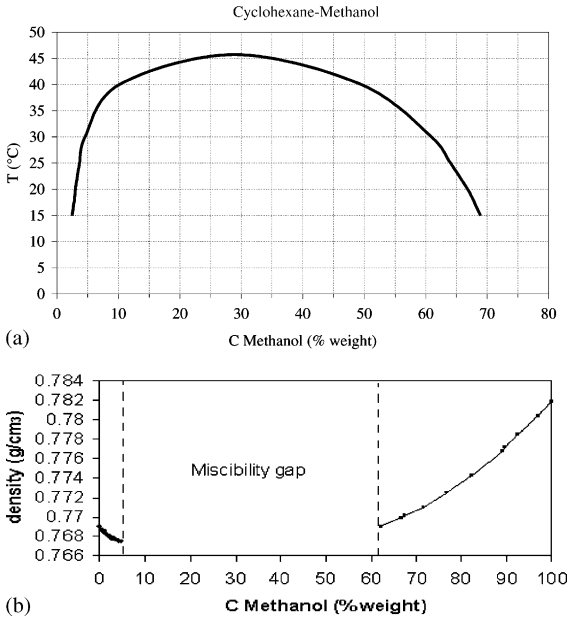

Fig. 5. Phase diagram (a) and density versus methanol concentration (b) for the cyclohexane–methanol system.

squeezed by the natural convection in the boundary layer close to the drop surface (see Figs. 8 and 9), increasing the solute gradient and the dissolution rate, compared to the purely diffusive situation.

The experiments have shown that when the initial volume of the droplet exceeds a critical value, depending on the experimental conditions (e.g. the temperature), after a transient time, the plume exhibits periodic oscillations that reveal a convective instability (Fig. 7). The experiments performed at ambient temperature (25 °C) show that the instability occurs only when the initial volume of the droplet is greater than 3 μl and that the oscillation period is an increasing function of the droplet diameter. Since the main objective of this work is to develop a numerical model for the simulation and the explanation of the dissolution process, details of the experimental results will be presented in a forthcoming paper.

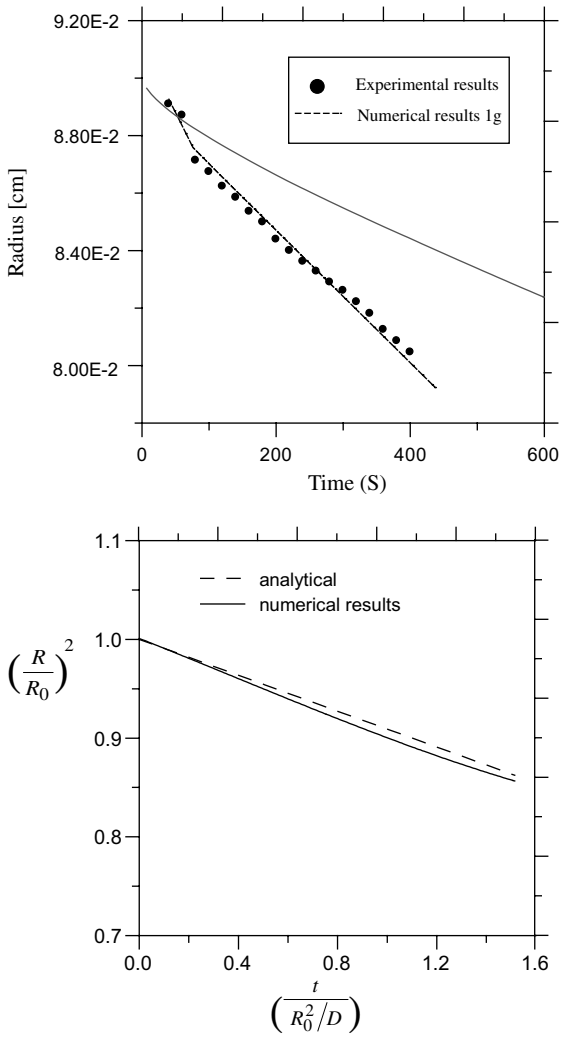

Fig. 6. Time evolution of the measured average drop radius and comparison with numerical results. The initial volume of the droplet (methanol) is 3 μl. The matrix is cyclohexane. (a) Comparison between numerical and experimental results; (b) comparison between numerical results, under zero gravity conditions, and the analytical solution.

3. Numerical model

3.1. Basic assumptions

Fig. 1 shows the geometry of the problem. A liquid drop is suspended in a liquid matrix. The liquid system (drop and matrix) is in a region of the phase diagram (T versus C) where it separates continuously into two phases, according to the equilibrium curve of Fig. 5. The droplet is anchored to the needle (or capillary tube) used to inject the liquid into the test cell. Since the temperature is almost uniform during the process, the pure liquids have constant phase density and transport coefficients. The drop is bounded by a spherical liquid/liquid interface whose radius changes in time due to the dissolution.

The thickness of the needle in the numerical simulations is negligible, but no slip conditions have been imposed along the axis to simulate the presence of the needle.

In order to evaluate the effect of the needle on the rate of dissolution, some preliminary computations have

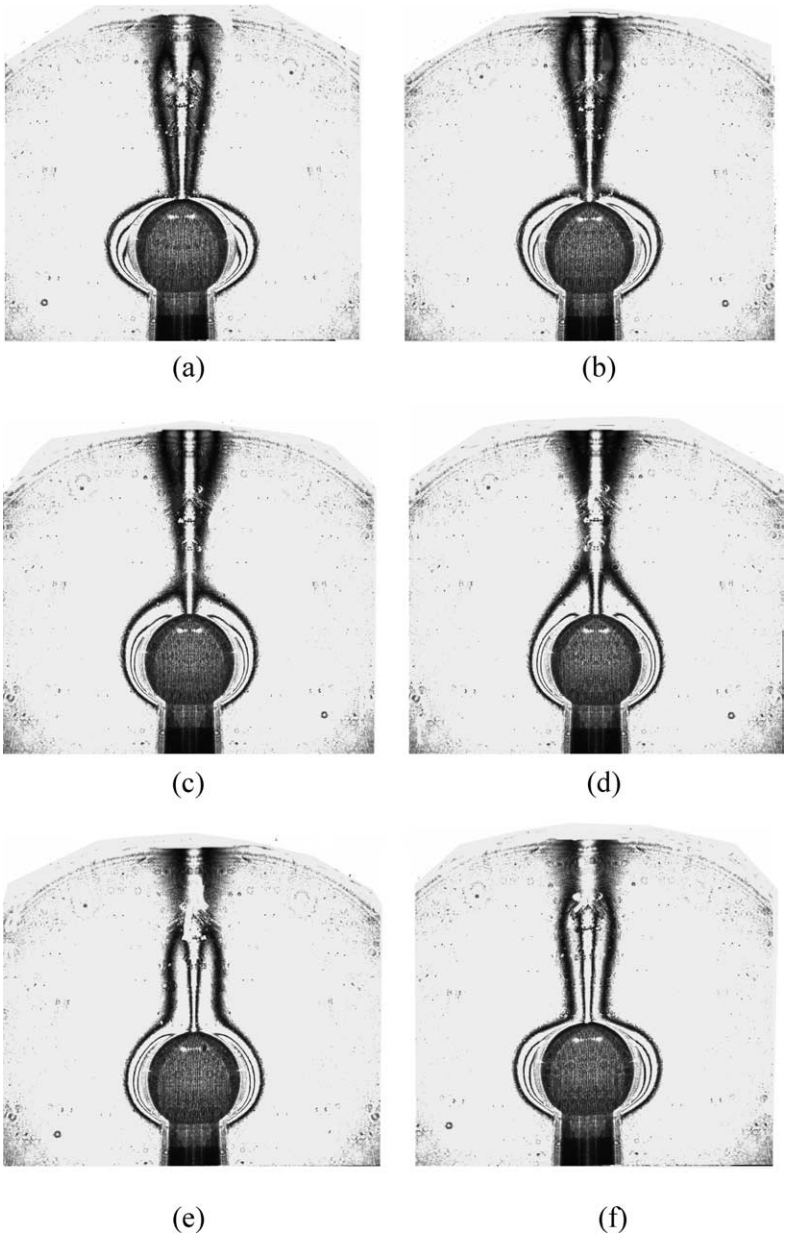

Fig. 7. Oscillatory instability of the axisymmetric plume rising from a drop of methanol dissolving in a cyclohexane matrix at ambient temperature. The initial volume of the drop is 5 μl. The images are taken at time intervals of 1 s.

been carried out taking into account its presence. A parametric study has shown that the influence of the needle on the results, for the diffusive case, scales according to the non-dimensional parameter $R_{cap}^2/(4R_{drop}^2)$ (where R_{drop} and R_{cap} are the radius of the drop and of the needle respectively). For the present case this parameter is 0.07, and therefore the needle perturbation on the dissolution rate is negligible. In addition, this influence becomes even less important if convection is taken into account because, in the convective regime, a solutal plume is created "above" the dissolving drop and the fluid near the needle is close to stagnation conditions.

The hypothesis of spherical surface is acceptable, as confirmed by the experiments, since the volume of the liquid drop is relatively small (few microliters) and the density difference between the two phases is very low, as discussed above.

3.2. Moving boundary method

In this section 'moving boundary' numerical methods are briefly outlined to point out similarities and differences with the numerical algorithm proposed here for the dissolution of drops in different liquids (dissolution of drops volume of fluid method—DDVFM). The numerical simulations of these problems require a discretization or nodalization to allow numerical treatment on computers. There are two fundamentally different approaches: Eulerian methods use a frame of reference (discretization grid or mesh, control volumes, etc.) fixed in space, and matter moving through this frame of reference. Lagrangian methods instead use a frame of reference (marker particles) fixed to and moving with the matter. The first method capable of modelling multiphase flow, separated by a moving interface, was the Marker and Cell (MAC) of Harlow and Welch [7]. This was in fact a combination of an Eulerian solution of the basic flow field, with Lagrangian marker particles attached to one phase to distinguish it from the other phase. While the staggered mesh layout and other features of MAC have become a model for many other Eulerian codes, the marker particles proved to be computationally too expensive and have been rarely used.

In the specific case of droplets growing or dissolving in a matrix of different liquid and in order to introduce novel numerical techniques, one must generally accomplish at least two things simultaneously: (a) determine the concentration fields in both liquid phases and (b) determine the position of the interface between the phases 1 and 2. According to the technique used to address (a) and (b), in principle the numerical procedures able to solve these problems can be divided in multiple or single region formulations.

Multiple region solutions are based on independent equations for each phase, coupled with suitable boundary conditions at the interface. This approach to the problem takes the point of view that the interface separating the bulk phases is a mathematical boundary of zero thickness where interfacial conditions are applied. These interfacial conditions couple to the concentration equations in the bulk and this system of equations and boundary conditions provide a means to address (a) and (b). Difficulties arise when this technique is employed since conditions on mass flux, velocity, and solubility evolution have to be accounted for in the vicinity of the interface. This effectively rules out the application of a fixed-grid numerical solution, as deforming grids or transformed co-ordinate systems are required to account for the position of the phase front.

Single region (continuum) formulations (or 'phase field' models) eliminate the need for separate equations in each phase, by establishing conservation equations in the whole field. From a theoretical point of view, the major advantage of the single region formulations is that they do not require the use of quasi-steady approximations, numerical remeshing and coordinate mapping. In a phase-field model, a phase-field variable ϕ changing in space and time is introduced to characterize the phase. In place of the 'sharp' transition from one phase to the other that would characterize the multiple region formulations, here the phase-field changes smoothly but rapidly through an interfacial region. The effect is a formulation of the free boundary problem that in principle does not require application of interfacial conditions at the unknown location of a phase boundary. This formulation is at the base of the most recent and popular methods used for moving boundary problems (volume of fluid VOF methods, see e.g. [8–10]; enthalpy methods, see e.g. [11–13]).

3.3. DDVFM—volume of fluid method for dissolving drops

The DDVFM is a single region formulation and allows a fixed-grid solution to be undertaken. It is therefore able to utilize standard solution procedures for the fluid flow and species equations directly, without resorting to mathematical manipulations and transformations.

The model is based on the mass balance equations. The diffusion of the species is governed by the equations (droplet phase 1, with $\phi = 1$, matrix phase 2 with $\phi = 0$):

$$\frac{\partial C_1}{\partial t} = \phi[-\underline{\nabla} \cdot (\underline{V} C_1) + D\nabla^2 C_1] \tag{1}$$

$$\frac{\partial C_2}{\partial t} = (1-\phi)[-\underline{\nabla} \cdot (\underline{V} C_2) + D\nabla^2 C_2] \tag{2}$$

The species equations (1) and (2) are solved in the computational domain including the droplet and the matrix. The presence of the terms ϕ and $(1-\phi)$ ensures in fact that each equation characterizes a different phase. At the initial instant both the phases are supposed to be at constant concentration ($C_{1(o)}$ and $C_{2(o)}$ respectively). The behaviour of the two phases is coupled through the equilibrium concentration values imposed on the two sides of the interface. On the interface ($0 < \phi < 1$), the concentrations must satisfy the equilibrium conditions:

$$C_1|_i = C_{1(e)} \tag{3}$$

$$C_2|_i = C_{2(e)} \tag{4}$$

Eqs. (3) and (4) behave as 'moving boundary conditions'. The transition region, defined by the mathematical conditions $|\underline{\nabla}\phi| \neq 0$, $0 < \phi < 1$, moves through the computational domain according to the behaviour of the different phases (i.e. according to the behaviour of ϕ).

The flow is governed by the continuity, and Navier–Stokes equations:

$$\underline{\nabla}\cdot\underline{V}=0 \tag{5}$$

$$\frac{\partial(\rho\underline{V})}{\partial t}=-\underline{\nabla}p-\underline{\nabla}\cdot[\rho\underline{V}\underline{V}]+\underline{\nabla}\cdot[\mu\underline{\nabla}\underline{V}]+\underline{F}_{\mathrm{g}} \tag{6}$$

where

$$\rho=\rho_{1(\mathrm{o})}\phi+\rho_{2(\mathrm{o})}(1-\phi) \tag{7a}$$

$$\mu=\mu_1\phi+\mu_2(1-\phi) \tag{7b}$$

The Boussinesq approximation for the density is adopted, so that the buoyancy term of Eq. (6) reads:

$$F_{\mathrm{g}}=g[\beta_1(C_1-C_{1(\mathrm{o})})]\phi+g[\beta_2(C_2-C_{2(\mathrm{o})})](1-\phi) \tag{7c}$$

where β_1 and β_2 are the solutal expansion coefficients related to the phases (1) and (2).

The tracking of the interface between the phases is accomplished by the solution of a special continuity integral equation for the volume of the liquid droplet taking into account the release or absorption of solute through the interface. The liquid drop is assumed to be a sphere of radius R increasing due to growth or decreasing due to dissolution. Using mass balance, one obtains for the time evolution of the radius:

$$\frac{\mathrm{d}R}{\mathrm{d}t}=\frac{D}{C_1|_i-C_2|_i}\frac{1}{S}\oint\left(\left.\frac{\partial C_2}{\partial n}\right|_i+\left.\frac{\partial C_1}{\partial n}\right|_i\right)\mathrm{d}l \tag{8}$$

where S is the surface of the droplet,

$$\frac{\partial C}{\partial n}=\underline{\nabla}C\cdot\hat{\underline{n}}=\alpha\frac{\partial C}{\partial x}+\beta\frac{\partial C}{\partial y} \tag{9}$$

$$\hat{\underline{n}}=-\frac{\underline{\nabla}\phi}{|\underline{\nabla}\phi|}=(\alpha,\beta) \tag{10a}$$

$$\alpha=-\frac{\partial\widehat{\phi}}{\partial x}\Bigg/\sqrt{\left(\frac{\partial\widehat{\phi}}{\partial x}\right)^2+\left(\frac{\partial\widehat{\phi}}{\partial y}\right)^2} \tag{11a}$$

$$\beta=-\frac{\partial\widehat{\phi}}{\partial y}\Bigg/\sqrt{\left(\frac{\partial\widehat{\phi}}{\partial x}\right)^2+\left(\frac{\partial\widehat{\phi}}{\partial y}\right)^2} \tag{11b}$$

The unit vector $\hat{\underline{n}}$ perpendicular to the interface results from the gradient of a smoothed phase field $\widehat{\phi}$, where the transition from one phase to the other takes place continuously over several cells (typically 4 or 5 for a grid having 200×200 points). The smoothed phase field $\widehat{\phi}$ is obtained by convolution of the unsmoothed field ϕ with an interpolation function. The interface orientation depends on the direction of the volume fraction gradient of the phase $\widehat{\phi}$ within the cell, and that of the neighbour cell (or cells) sharing the face in question. Depending on the interface's orientation and on the side (phase (1) or phase (2)) on which computations are performed, concentration gradients are discretized by forward or backward schemes.

For $C=C_1$, $\partial C/\partial x=(C_{i,j}-C_{i-1,j})/\Delta x$ if $\alpha>0$, $\partial C/\partial x=(C_{i+1,j}-C_{i,j})/\Delta x$ if $\alpha<0$; for $C=C_2$, $\partial C/\partial x=(C_{i+1,j}-C_{i,j})/\Delta x$ if $\alpha>0$, $\partial C/\partial x=(C_{i,j}-C_{i-1,j})/\Delta x$ if $\alpha<0$ (similar relationships hold for the concentration gradient along y).

Then the distribution of the phase variable ϕ is defined according to the radius of the drop at the new instant $(n+1)$:

$$r<R,\quad \phi=1 \tag{12a}$$

$$r>R,\quad \phi=0 \tag{12b}$$

Eqs. (1), (2), (5), (6) and (8) represent a system of four partial differential equations and one ordinary differential equation whose solution governs the non-linear behaviour of the physical system under investigation.

Note that the present mathematical model and related numerical technique can be regarded as a very hybrid volume of fluid method. In the "classical" VOF methods, the phase field variable ϕ is 'advected' solving an appropriate partial differential transport equation; this formulation has been often used for the solution of typical problems dealing with the migration of bubbles or drops in liquids. It relies on the fact that the fluids are not interpenetrating. For the present method the equation governing the evolution of ϕ comes from mass balance conditions rather than from transport. Moreover interpenetration of the different fluids is allowed according to the coupled behaviour of Eqs. (1), (2) and (8).

Eq. (8) moreover provides the necessary coupling among the species and momentum equations. The density and the dynamic viscosity of the liquid in Eq. (6) in fact are computed according to the instantaneous distribution of ϕ. Further coupling between the species and momentum equations is due to the volume force term (Boussinesq approximation) in Eq. (6).

3.4. Discretization and solution

Eqs. (1), (2), (5), and (6) subjected to the initial and boundary conditions are solved numerically in primitive variables by a control volume method. The domain is discretized with a cylindrical axisymmetric uniform mesh and the flow field variables defined over a staggered grid. Forward differences in time and upwind schemes in space (second order accurate) are used to discretize the partial differential equations.

The computation of the velocity field at each time step is split into two substeps. In the first, an approximate non-solenoidal velocity field $\underline{V}^*$ which corresponds to the correct vorticity of the field is computed at time $(n+1)$ neglecting the pressure gradient term in the momentum Eq. (6). In the second substep, the pressure field is computed by solving the equation resulting from the divergence of the momentum equation taking into account Eq. (5):

$$\nabla^2 p = \frac{1}{\Delta t}\underline{\nabla}\cdot\underline{V}^* \tag{13}$$

This equation is solved with a successive over relaxation (SOR) iterative method. For further details on the numerical method see e.g. [14–16]. On the solid walls and on the symmetry axis the $\partial P/\partial n = 0$ condition is imposed.

Finally, the correct solenoidal velocity field is updated using the computed pressure field to account for continuity:

$$\underline{V}^{n+1} = \underline{V}^* - \Delta t\underline{\nabla}p^n \tag{14}$$

4. Results and discussion

Fig. 8 shows the computed evolution of the concentration and flow field patterns at the beginning of the dissolution process. The numerical results refer to a droplet of methanol dissolving into a matrix of cyclohexane at ambient temperature. The initial volume of the droplet is 3 μl with a diameter of 1.8 mm. The computations are carried out considering normal (Earth) gravity and therefore buoyancy effects. The results of Fig. 8 show the streamlines and the concentration of methanol around the dissolving droplet at different times. The plume starts rising and after $t = 100$ s fully developed velocity and concentration fields are established.

Fig. 6a shows the computed time dependence of the average drop radius. The initial volume of the drop is the same as in Fig. 8 (3 μl). The numerical simulations have been carried out in the two cases: (a) zero gravity conditions (i.e. zero buoyancy); (b) Earth gravity conditions (i.e. in the presence of buoyancy convection). The numerical results show that buoyancy induced convection increases the droplet dissolution, in comparison with the purely diffusive situation. The volume of the drop decreases more rapidly as time increases, and better correlation with the experimental results is achieved if convection is taken into account.

The numerical results corresponding to zero gravity (purely diffusive) conditions have been compared in Fig. 6b with the analytical solution $R^2 = R_0^2 - D\frac{c_m - c_{2(e)}}{c_{2(e)} - c_{1(e)}}t$, obtained by the integration of the diffusion equation assuming a spherical droplet dissolving in an unbounded medium at constant concentration. The droplet radius thus changes as the square root of time [1].

Fig. 6b shows the time profiles of the quadratic dissolution (R^2/R_0^2) versus the non-dimensional time (tD/R_0^2). The good correlation between the results of the numerical model and the analytical solution provides a satisfactory validation of the numerical method on this specific problem.

As discussed in Section 2, the experiments performed with binary liquid–liquid systems have shown that the phenomena under investigation may exhibit "stable" rising solutal plumes (created above the dissoving drop) or "pulsating" jets showing time-dependent oscillatory behaviour. The numerical results confirm that, for sufficiently small values of the initial volume of the drop, the convection in the liquid column is laminar and steady, but if this initial volume exceeds certain critical values, the liquid motion undergoes a transition to an oscillatory axisymmetric complex flow pattern. Note that the experimental fringes around the dissolving drop in the observation plane are defined curves whose shape approximately looks like two symmetric folds disposed on the left and right sides of the drop (see Fig. 7). The pulsating behaviour consists in "quasi-periodic" expansions and contractions of the two folds. The velocity and the concentration fields are symmetric and the time-dependence is observed as a synchronous pulsation of these symmetrical folds (they travel axially up and down). The periodic motion is not confined however to the zone close to the drop surface and affects also the behaviour of the plume carrying methanol towards the top of the test cell. According to the experiments, the numerical results show that the instability leads somehow to a "periodic release" of a "packet" of lighter fluid in the plume, with a periodic expansion of the diameter of the rising jet (Figs. 9 and 10). It appears as a disturbance travelling towards the top (i.e. a perturbation of the solutal and flow field rising along the core of the plume).

The mathematical model and the associated numerical algorithm have proven to be able to "capture" the complex time-dependent phenomena and to provide information and data about the intrinsic nature of the instability.

It must be pointed out that the oscillations do not exhibit very regular and repeatable oscillations; rather they are characterized by a "quasi-periodic/non-periodic" behaviour. This aspect is revealed both by the experimental and numerical results. Therefore, the definition of a well-defined "frequency" for the phenomena is almost meaningless. However, the numerical code captures the underlying physical mechanisms responsible for the onset of oscillatory instability and the "average" experimental and numerical frequencies agree in terms of order of magnitude (the experimental oscillation period is about 7 s, the numerical one is about 9 s, see the time intervals in the Figs. 7 and 9).

Computations obtained by "switching off" the surface tension effects have proved that the phenomena under investigation are driven by the buoyancy (gravitational) effect only, whereas the solutal Marangoni flow does not seem to play a critical role in the onset of the flow instability.

Fig. 8 show the presence of a large toroidal convection roll wrapped around the solutal jet. The instability is hydrodynamic in nature (the solutal field simply acts

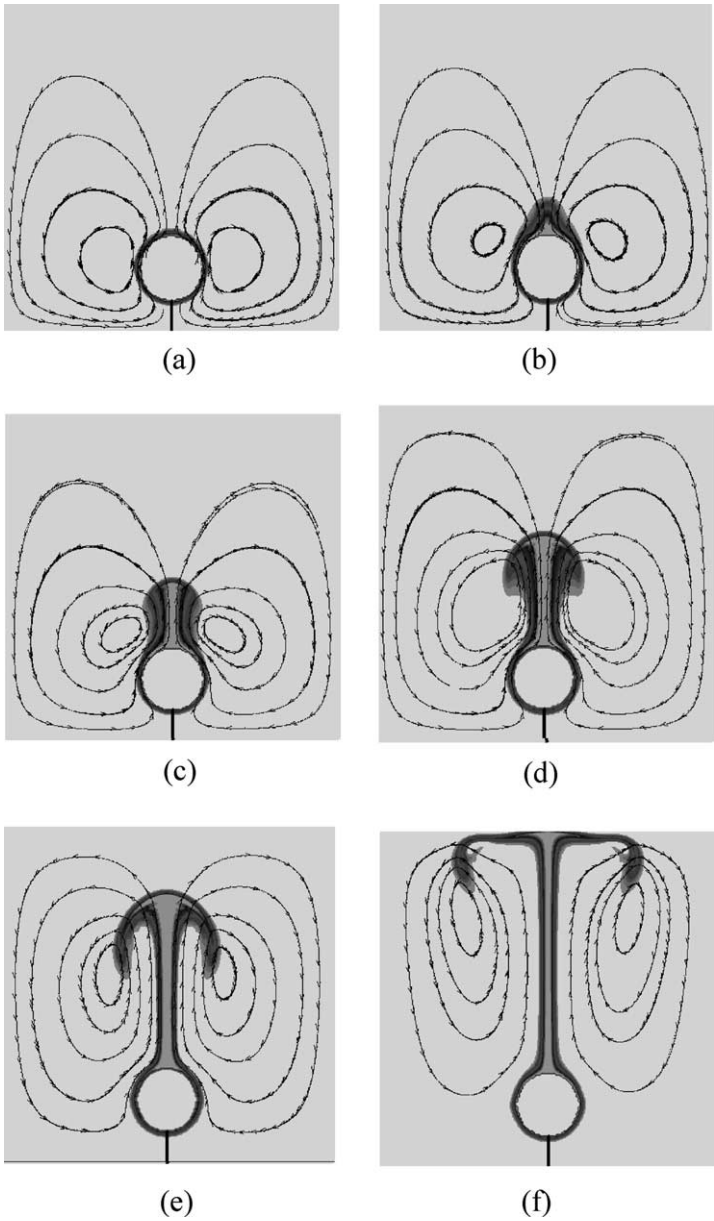

Fig. 8. Computed evolution of the concentration and flow field patterns at the beginning of the dissolution process (droplet of methanol dissolving into a matrix of cyclohexane at ambient temperature, initial volume of the droplet 3 μl, $V_{max} = 5.4 \times 10^{-2}$ cm/s). The time intervals are 8 seconds.

as a "driving force" for the velocity field). When the velocity exceeds a critical value, bifurcation to oscillatory flow occurs. This explains why the instability occurs only if a certain initial value of the drop volume is exceeded, whereas the flow exhibits stable solutal rising plumes in the case of small initial volumes; the maximum velocity in the core of the rising plume in fact depends on the flow rate of methanol through the drop interface; in turn this flow rate depends on the surface area of the drop and therefore on its radius.

With regard the nature of the instability, the phenomena here discussed exhibit surprising similarities with oscillatory instabilities of candle flames and of buoyant plumes (see [17–20]). Cetegen [19] carried out experimental studies dealing with the instabilities and flow transitions of buoyant plumes/jets of gas mixtures. The case of a plume of helium or helium/air mixture, originating from a large axisymmetric nozzle with low velocity, was investigated. The experiments pointed out toroidal vortex formation as a result of rapid buoyant

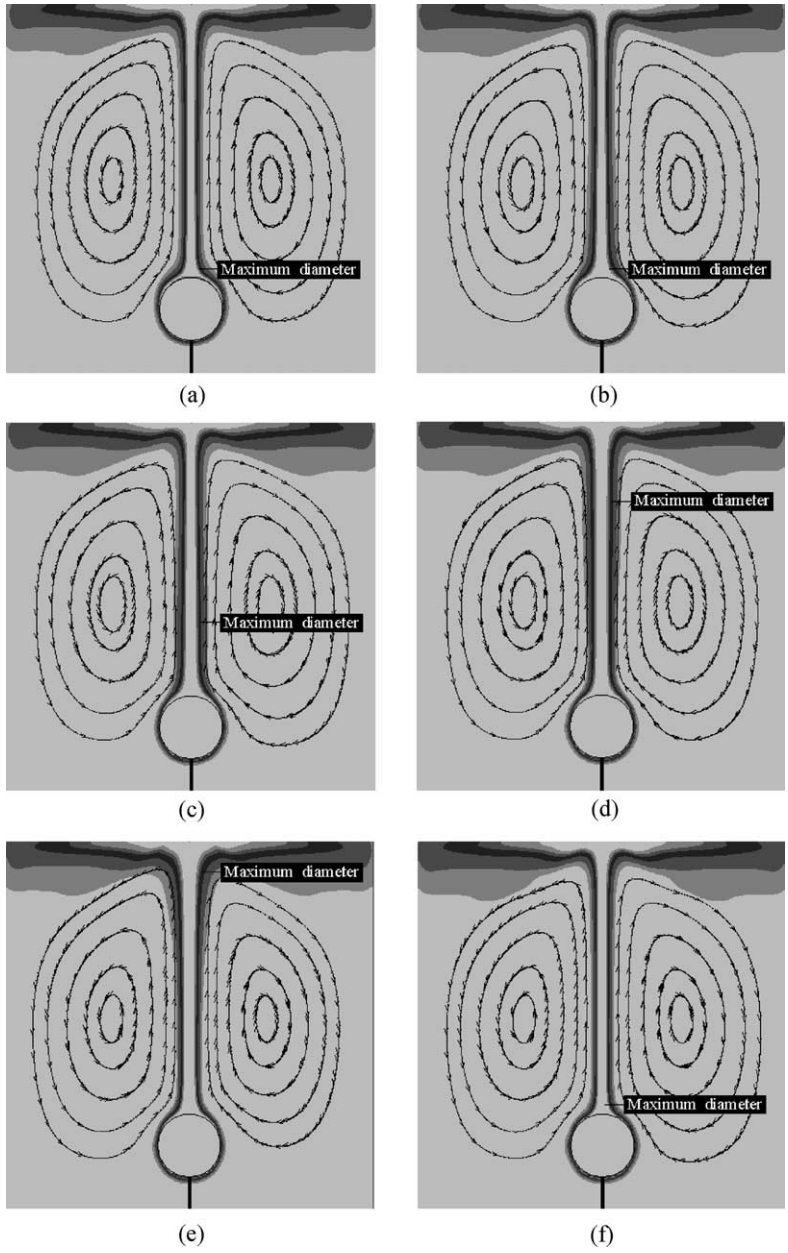

Fig. 9. Computed evolution of the unstable solutal plume: concentration and flow field patterns for a 3 μl droplet of methanol dissolving into a matrix of cyclohexane at ambient temperature ($V_{max} = 5.4 \times 10^{-2}$ cm/s). The time intervals are 1.8 seconds.

acceleration of light plume fluid in heavier more or less quiescient surroundings. In particular, it was found that these plumes may undergo quasi-periodic oscillations with a macroscopic behaviour very similar to that described in the present work. As the buoyant fluid exits the nozzle, plume boundary contracts towards the plume centerline as a result of buoyant acceleration, due to the hydrostatic pressure field and the condition imposed by the mass conservation. The plume undergoes oscillations close to the nozzle lip, similar to the oscillations observed in the present study close to the drop surface. Moreover, similar to the present case of solutal plumes, Cetegen [19] found that only in some cases the buoyant plumes exhibit periodic oscillations. The onset of oscillations is in fact a function of the nozzle diameter, of the nozzle exit velocity and of the density ratio between the

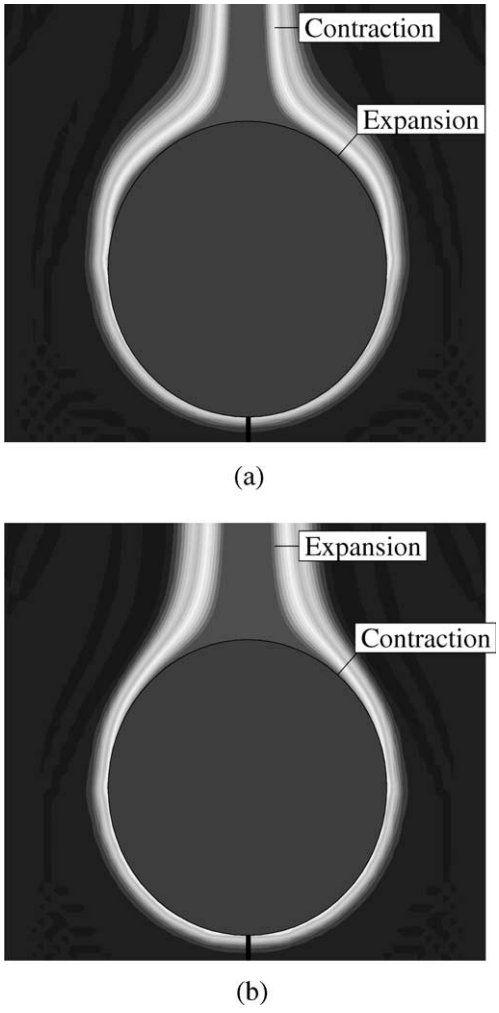

Fig. 10. Computed pulsating behaviour close to the surface of the dissolving drop (figures (a) and (b) refer to the maximum and to the minimum of an oscillation period respectively). (a) Contraction of the plume diameter, expansion of the two surface folds. (b) Contraction of the two surface folds, expansion of the plume diameter.

plume and the surrounding ambient medium [19]. In the present case, instability occurs only if a critical initial volume of the drop is exceeded.

Cetegen and Kasper [18] provided a very interesting explanation of these phenomena: the mechanism leading to the periodic oscillatory state of the flow field is connected with the highly unstable (Rayleigh–Taylor) density stratification in the sharply contracting region of the flow just above the nozzle exit. According to the present numerical simulations, the same mechanism occurs in the solutal flow, since unstable density stratification occurs just above the dissolving drop. Note that similarities exist also with the behaviour of candle flames that exhibit an oscillatory motion often referred to as "puffing" [17]. Typically these oscillations result in formation of large-scale (of the order of burner diameter) flaming vortical structures at a short distance from the burner surface. These structures significantly modify the downstream flame behaviour as they rise through the flame and finally burnout near the flame top.

Again, the behaviour is very similar to the periodic "release" of packets of fluid in the rising jet generated above the dissolving droplets. The perturbation in the solutal jet diameter originated at the drop surface rises along the core of the jet and vanishes at the top.

In summary, "puffing" in isothermal helium plumes, in candle flames and in the present case of droplet dissolution are all related to buoyant instabilities. In the case of helium plumes, the driving force is the pressure gradient between the helium reservoir and the ambient. For candle flames the driving force is the heat released in the core of the flame, due to the combustion process. In the present case, the driving force for the oscillatory instability is the concentration gradient due to the dissolution of the droplet placed at the bottom of the test cell. The dissolution provides continuously lighter fluid that is carried up due to the buoyancy forces.

5. Conclusions

The behaviour of solutal plumes rising around a droplet of methanol during the dissolution in a matrix of cyclohexane has been investigated with a numerical model. Similar to the experiments, the numerical results show that that the plume undergoes oscillations and contractions towards the plume centerline. The mechanism is very similar to other oscillatory instabilities of candle flames or of isothermal buoyant jets.

Future studies will be dedicated to the parametric analysis of the puffing phenomenon of dissolving droplets, either experimentally or numerically.

Acknowledgements

The authors would like to thank Mr. Nicola di Francescantonio for the experiments performed in the frame of his thesis in Aerospace Engineering.

References

[1] Decomposition, Phase separation, Solidification of immiscible liquid alloys, in: L. Ratke (Ed.), Immiscible Liquid Metals and Organics, Proceedings of an International Workshop organized by the ESA Expert Working Group, "Immiscible alloys" held in the Physikzentrum, Bad Honnef 1992, Germany, 1992, pp. 3–34.

[2] B. Prinz, A. Romero, New casting process for hypermonotectic alloys, in: L. Ratke (Ed.), Immiscible Liquid Metals

and Organics, Proceedings of an International Workshop organized by the ESA Expert Working Group, "Immiscible Alloys" held in the Physikzentrum, Bad Honnef 1992, Germany, 1992, pp. 281–289.

[3] N.O. Young, J.S. Goldstein, M.J. Block, The motion of bubbles in a vertical temperature gradient, J. Fluid Mech. 6 (1959) 350–360.

[4] D. Agble, M.A. Mendes Tatsis, The effect of surfactants on interfacial mass transfer in binary liquid–liquid systems, Int. J. Heat Mass Transfer 43 (2000) 1025–1034.

[5] E. Susana Perez de Ortiz, H. Sawistoski, Interfacial instability of binary liquid–liquid systems. I. Stability analysis, J. Chem. Eng. Sci. 28 (1973) 2051–2061.

[6] The Physical–Chemical Constants of Binary systems, Interscience, New York, 1959.

[7] F.H. Harlow, J.E. Welch, Numerical calculation of time-dependent viscous incompressible flow with free surface, Phys. Fluids 8 (1965) 2182–2189.

[8] C.W. Hirt, B.D. Nichols, Volume of fluid (VOF) method for the dynamics of free boundaries, J. Comput. Phys. 39 (1981) 201–225.

[9] S. Osher, J.A. Sethian, Fronts propagating with curvature-dependent speed: algorithms based on Hamilton–Jacobi formulations, J. Comput. Phys. 79 (1988) 12–49.

[10] D. Gueyffier, J. Li, A. Nadim, S. Scardovelli, S. Zaleski, Volume of fluid interface tracking with smoothed surface stress methods for three-dimensional flows, J. Comput. Phys. 152 (1999) 423–456.

[11] W.D. Bennon, F.P. Incropera, A continuum model for momentum, heat and species transport in binary solid–liquid phase change systems—I. Model formulation, Int. J. Heat Mass Transfer 30 (10) (1987) 2161–2170.

[12] W.D. Bennon, F.P. Incropera, A continuum model for momentum, heat and species transport in binary solid–liquid phase change systems—II. Application to solidification in a rectangular cavity, Int. J. Heat Mass Transfer 30 (10) (1987) 2171–2187.

[13] V.R. Voller, C. Prakash, A fixed grid numerical modelling methodology for convection–diffusion mushy region phase-change problems, Int. J. Heat Mass Transfer 30 (8) (1987) 1709–1719.

[14] R. Monti, R. Savino, M. Lappa, S. Tempesta, Behaviour of drops in contact with liquid surfaces at non wetting conditions, Phys. Fluids 10 (11) (1998) 2786–2796.

[15] M. Lappa, Strategies for parallelizing the three-dimensional Navier–Stokes equations on the Cray T3E, Sci. Supercomput. CINECA 11 (1997) 326–340.

[16] M. Lappa, R. Savino, Parallel solution of three-dimensional Marangoni flow in liquid bridges, Int. J. Numer. Meth. Fluids 31 (1999) 911–925.

[17] B.M. Cetegen, T.A. Ahmed, Experiments on the periodic instability of buoyant plumes and pool fires, Combust. Flame 93 (1993) 157–184.

[18] B.M. Cetegen, K.D. Kasper, Experiments on the oscillatory behaviour of buoyant plumes of helium and helium-air, Phys. Fluids 8 (11) (1996) 2974–2984.

[19] B.M. Cetegen, Behaviour of naturally oscillating and periodically forced axisymmetric buoyant plumes of helium and helium-air mixtures, Phys. Fluids 9 (12) (1997) 3742–3753.

[20] B.M. Cetegen, Y. Dong, C. Soteriou, Experiments on stability and oscillatory behaviour of planar buoyant plumes, Phys. Fluids 10 (7) (1998) 1658–1665.